Protein Science (1993), *2*, 1274–1284. Cambridge University Press. Printed in the USA.

Refinement of the structure of human basic fibroblast growth factor at 1.6 Å resolution and analysis of presumed heparin binding sites by selenate substitution

A. ELISABETH ERIKSSON,[1,3] LAWRENCE S. COUSENS,[2,4] AND BRIAN W. MATTHEWS[1]

[1] Institute of Molecular Biology, Howard Hughes Medical Institute and Department of Physics, University of Oregon, Eugene, Oregon 97403

[2] Chiron Corporation, 4560 Horton Street, Emeryville, California 94608

(RECEIVED February 23, 1993; REVISED MANUSCRIPT RECEIVED May 10, 1993)

Abstract

The three-dimensional structure of human basic fibroblast growth factor has been refined to a crystallographic residual of 16.1% at 1.6 Å resolution. The structure has a Kunitz-type fold and is composed of 12 antiparallel β-strands, 6 of which form a β-barrel. One bound sulfate ion has been identified in the model, hydrogen bonded to the side chains of Asn 27, Arg 120, and Lys 125. The side chain of Arg 120 has two conformations, both of which permit hydrogen bonds to the sulfate. This sulfate binding site has been suggested as the binding site for heparin (Eriksson, A.E., Cousens, L.S., Weaver, L.H., & Matthews, B.W., 1991, *Proc. Natl. Acad. Sci. USA 88*, 3441–3445). Two β-mercaptoethanol (BME) molecules are also included in the model, each forming a disulfide bond to the S^{γ} atoms of Cys 69 and Cys 92, respectively. The side chain of Cys 92 has two conformations of which only one can bind BME. Therefore the BME molecule is half occupied at this site.

The locations of possible sulfate binding sites on the protein were examined by replacing the ammonium sulfate in the crystallization medium with ammonium selenate. Diffraction data were measured to 2.2 Å resolution and the structure refined to an *R*-factor of 13.8%. The binding of the more electron-dense selenate ion was identified at two positions. One position was identical to the sulfate binding site identified previously. The second selenate binding site, which is of lower occupancy, is situated 5.6 Å from the first. This ion is hydrogen bonded by the side chain of Lys 135 and Arg 120. Thus the side chain of Arg 120 binds two selenate ions simultaneously. It is suggested that the observed second selenate binding site should also be considered as a possible binding site for heparin, or that both selenate binding sites might simultaneously contribute to the binding of heparin.

Keywords: interleukins; Kunitz fold; oncogenes; receptors; sulfate binding; trypsin inhibitor

Basic fibroblast growth factor (bFGF; Abraham et al., 1986) is one of the seven currently known members of the FGF family that includes acidic FGF (aFGF; Jaye et al., 1986), int-2 gene product (int-2; Dickson & Peters, 1987), hst/kFGF (Delli-Bovi et al., 1987; Yoshida et al., 1987), FGF-5 (Zhan et al., 1988), FGF-6 (Marics et al., 1989), keratinocyte growth factor (KGF; Finch et al., 1989), and the actin-binding protein hisactophilin (Habazettl et al., 1992). It has been suggested that the nomenclature of all members of the family should include the designation "FGF" (for details see Baird & Klagsbrun [1991]). Thus, aFGF and bFGF can also be identified as FGF 1 and FGF 2. Here we retain the commonly used nomenclature and designate human basic fibroblast growth factor as hbFGF. The amino acid sequence identity of the members within the FGF family is 30–55%.

Functions associated with members of the FGF family include the stimulation of cell migration and cell differentiation for a variety of different cell types. Some members are oncogenes (int-2, hst/kFGF, FGF-5, and FGF-6) and both aFGF and bFGF show angiogenic properties (Folkman & Klagsbrun, 1987), which suggests possible roles in tumor growth. In addition, bFGF and an FGF receptor have been identified in *Xenopus*, where FGF is a

Reprint requests to: Brian W. Matthews, Institute of Molecular Biology, Howard Hughes Medical Institute, University of Oregon, Eugene, Oregon 97403.

[3] Present address: Institute of Molecular Biology, Uppsala University, Uppsala Biomedical Center, Box 590, 751 24 Uppsala, Sweden.

[4] Present address: ICOS Corp., 22021 20th Avenue SE, Bothell, Washington 98021.

potent inducer of mesoderm formation in developing embryos (Kimelman et al., 1988; Musci et al., 1990). Both aFGF and bFGF are thought to interact with heparin, a naturally occurring, highly sulfated glycosaminoglycan (Maciag et al., 1984; Shing et al., 1984; Kan et al., 1993; Nurcombe et al., 1993). Although the biological activity of aFGF is mediated by heparin, the activity of bFGF does not appear to be mediated or potentiated by the proteoglycan (Thornton et al., 1983; Shreiber et al., 1985; Terranova et al., 1985; Gospodarowicz & Cheng, 1986).

The mechanisms by which FGFs promote their biological responses are poorly understood. To date, four members of the FGF receptor gene family have been identified. Also, further diversity can be generated by alternative splicing of receptor genes (Miki et al., 1992; Vainikka et al., 1992). Both aFGF and bFGF react with a common receptor on the cell surface (Neufeld & Gospodarowicz, 1986). The response probably involves both activation of a tyrosine kinase domain possessed by the receptors (Huang et al., 1986; Coughlin et al., 1988; Friesel et al., 1989) and phosphorylation of phospholipase C-γ (Burgess et al., 1990a).

We have previously reported the three-dimensional structure of hbFGF at 2.2 Å resolution (Eriksson et al., 1991). The present report includes a description of the refined structure at 1.6 Å resolution. To verify the presence of a presumed sulfate and heparin binding site on the protein, we have also determined the structure of bFGF using crystals soaked in a selenate rather than sulfate-containing solution.

Independent structure determinations of aFGF and hbFGF have been reported by Ago et al. (1991), Zhang et al. (1991), and Zhu et al. (1991).

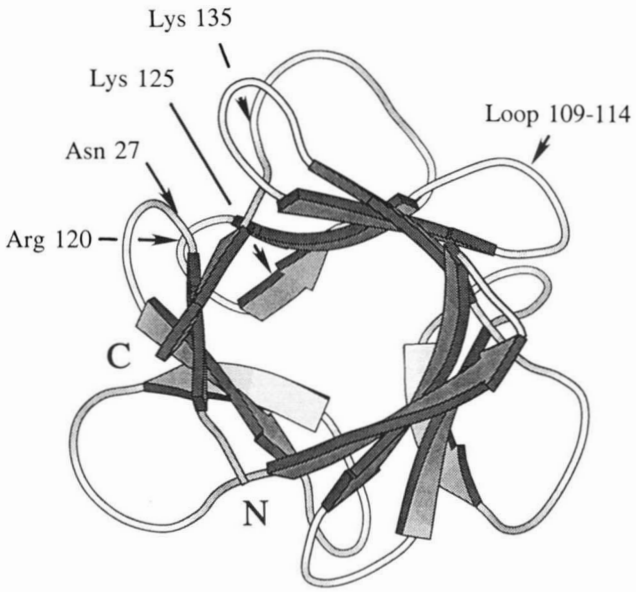

Fig. 1. Ribbon drawing of human basic fibroblast growth factor (hbFGF) made with the graphics program MOLSCRIPT (Kraulis, 1991). The locations of the amino acids that participate in sulfate and/or selenate binding (Asn 27, Arg 120, Lys 125, and Lys 135) are indicated. Also shown is the loop consisting of residues 109–114 that is included within the putative receptor-binding peptide (residues 106–115) identified by Baird et al. (1988).

Results and discussion

Overall structure

The overall folding of the refined hbFGF structure (Fig. 1; Kinemage 1) is essentially unchanged relative to that described previously (Eriksson et al., 1991). The structure is built of 12 antiparallel β-strands with a fold very similar to that of both interleukin (IL)-1α (Einspahr et al., 1990; Graves et al., 1990) and IL-1β (Priestle et al., 1988, 1989; Finzel et al., 1989), as well as members of the Kunitz-type soybean trypsin inhibitor family (Sweet et al., 1974; McLachlan, 1979; Onesti et al., 1991) and the bifunctional proteinase K/α-amylase inhibitor from wheat (Zemke et al., 1991). The characteristic features of the folding of members of the Kunitz family have been thoroughly described (McLachlan, 1979; Murzin et al., 1992).

The structure can be divided into three submotifs each consisting of four antiparallel β-strands. The overall fold can then be described as a trigonal pyramid in which the three sides are built of the top two β-strands from each motif and the strands together form a β-sheet barrel of six antiparallel β-strands. The base of the pyramid is built of six additional β-strands, consisting of the bottom two β-strands from each motif and closing one end of the barrel. Thus, a threefold repeat is observed in the folding of the polypeptide chain and a pseudo-threefold axis passes through the center of the base of the molecule and extends through the apex of the pyramid (see Fig. 1). There are also local threefold axes within each of the three sides of the pyramid. A buried water molecule is situated on each of these three local axes and forms hydrogen bonds to the threefold-related strands that come together around each threefold axis (Fig. 2; Kinemage 2). The inside of the β-barrel is completely filled with hydrophobic side chains plus the one somewhat polar residue, Tyr 106. The side chain of Tyr 106 is completely buried, but the phenolic hydroxyl forms a hydrogen bond to the side chain of Glu 96, which in turn contacts bulk solvent.

We have previously compared the α-carbon backbone of bFGF with that of human IL-1β (Priestle et al., 1989). Based on 50 residues whose α-carbons superimposed with a root mean square (rms) discrepancy of 0.5 Å (Rossmann & Argos, 1975), we proposed an alignment of the amino acid sequences of bFGF and IL-1β (Eriksson et al., 1991). At that point we were not concerned that every residue in the FGF structure should be individually aligned with every other residue in IL-1β. Rather, we wanted to show the overall alignment of the respective sequences as suggested by the structural superposition of the β-sheet strands and to contrast these alignments with the very different alignment that had been proposed previously on

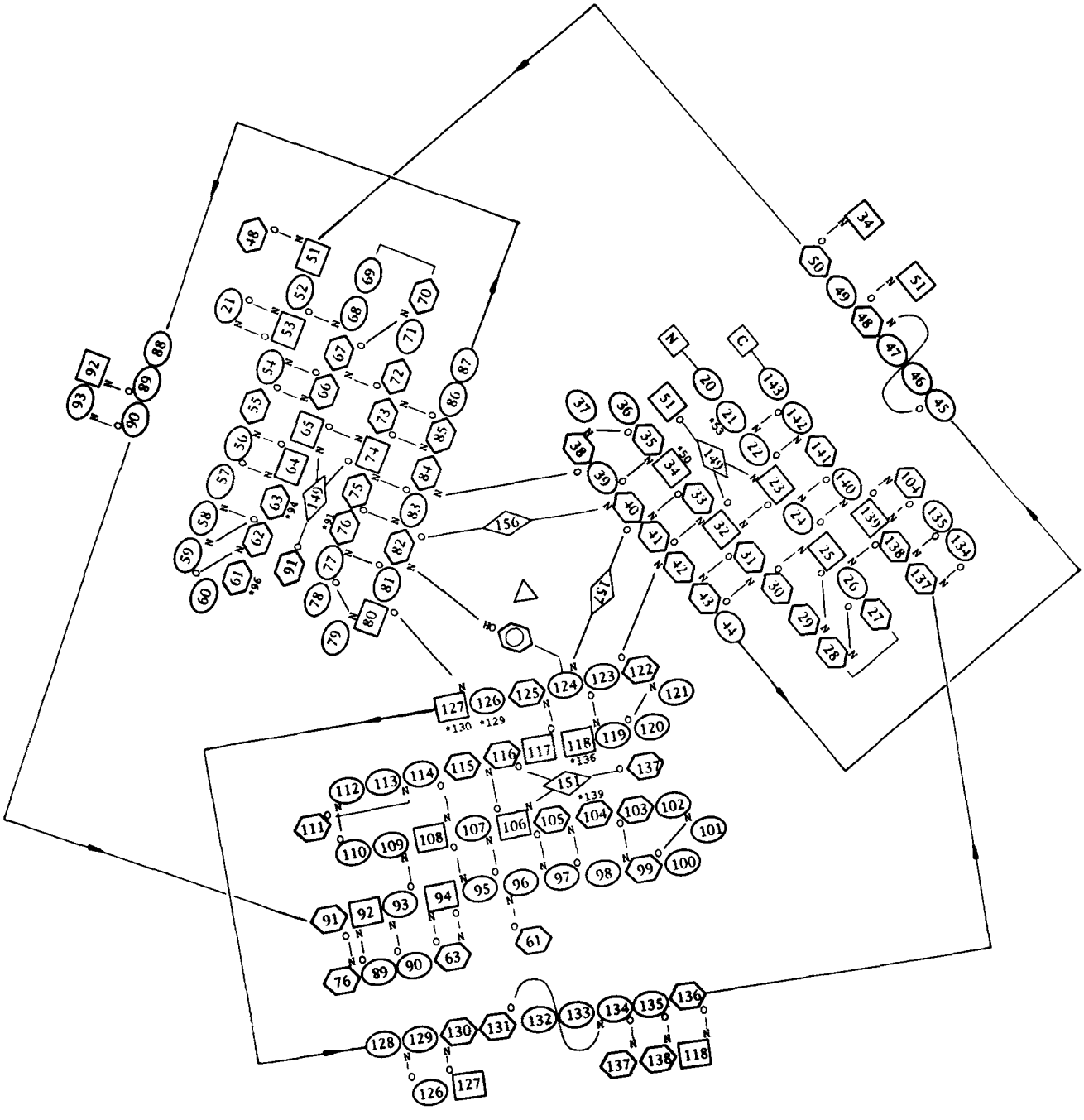

Fig. 2. Main-chain hydrogen-bonding scheme of hbFGF defined by DSSP (Kabsch & Sanders, 1983). The cutoff value for the binding energy is −1.0 kcal/mol for hydrogen bonds. ◇, Buried water molecule, which stabilizes secondary structure; *, hydrogen-bonding partner. The surface accessibility of different residues is illustrated as: □, 0 Å^2; ⬭, 1-50 Å^2; and ⬭, >50 Å^2.

the basis of sequence comparison alone. We did not attempt a residue-by-residue comparison of the respective backbones of the two molecules to ensure that the rest of the sequences were aligned to achieve optimal structural overlap. Therefore it is not surprising that some discrepancies in detail exist between our alignment and the structural alignments suggested by others (Zhang et al., 1991; Zhu et al., 1991). In order to resolve these discrepancies, insofar as possible, we have made a more careful comparison of the two structures, resulting in the revised sequence alignment presented in Figure 3. This sequence alignment is now in closer agreement with those of Zhang et al. (1991) and Zhu et al. (1991), although some discrepancies still exist, mostly due to the subjective interpretations that have to be made regarding the optimal alignment within the loop regions.

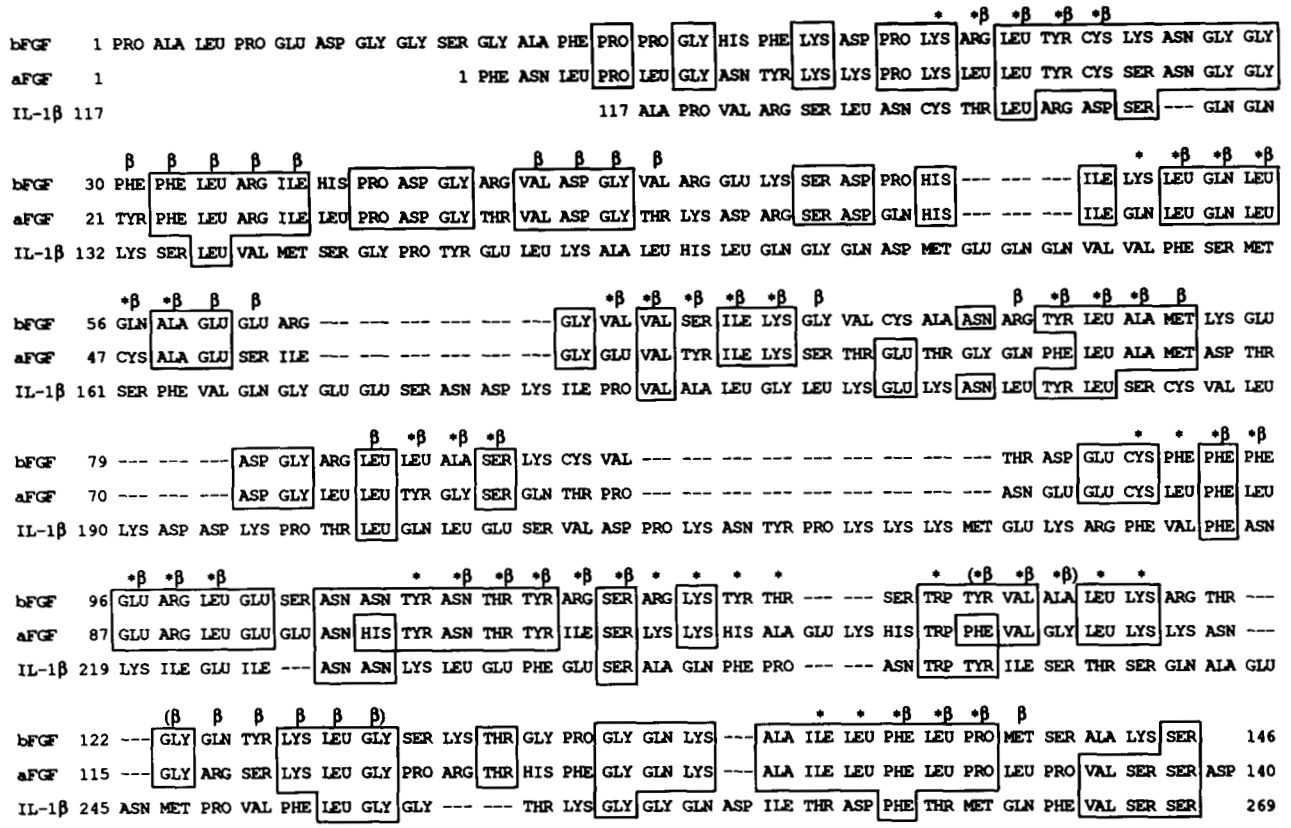

Fig. 3. Alignment of the amino acid sequences of hbFGF (Abraham et al., 1986) (sequence numbered to correspond to bovine bFGF; Esch et al., 1985) and interleukin (IL)-1β (Gimenez-Gallego et al., 1985; Thomas & Gimenez-Gallego, 1986) suggested by the correspondence between their three-dimensional crystal structures (Priestle et al., 1989; Eriksson et al., 1991; this work). The sequence of bovine aFGF is also included (Gimenez-Gallego et al., 1985). The 50 residues whose α-carbons structurally superimpose with an rms discrepancy of 0.52 Å are indicated with asterisks. Residues in bFGF that are indicated by the algorithm of Kabsch and Sanders (1983) as having a β-sheet conformation are indicated (β). There are 10 such "β-sheet strands" shown in the figure. There are two additional segments, indicated (β ... β) that do not fulfill the Kabsch and Sanders criteria for β-sheet strands but form the 10th and 11th of the 12 β-strands that comprise the overall framework of the bFGF and IL-1β structures. These segments have been realigned relative to Eriksson et al. (1991) to now comprise residues 115–117 and 122–127.

According to the sequence alignment shown in Figure 3, there is only a 13% sequence identity between bFGF and IL-1β (18 out of 134). Among the 50 residues that superimpose within 0.5 Å, 9 are identical (18%). The close correspondence of the backbone core, notwithstanding low sequence homology, can presumably be attributed to the interlocking β-sheet network that characterizes these structures. This network forms a scaffold that is defined by backbone–backbone rather than side-chain–side-chain or side-chain–backbone interactions and therefore may be relatively insensitive to amino acid substitution.

β-Mercaptoethanol binding

There are four cysteine residues in hbFGF, located at positions 25, 69, 87, and 92 (Abraham et al., 1986). Cys 25 and Cys 92 are highly conserved in different members of the FGF family (Burgess & Maciag, 1989; Finch et al., 1989; Marics et al., 1989). Two β-mercaptoethanol (BME) molecules, present in the crystallization medium, were identified in the bFGF structure forming disulfide bridges to Cys 69 and Cys 92, respectively. The BME molecule bound to Cys 69 appears to be fully occupied and has geometry typical of a normal disulfide linkage. The distance between the two sulfurs is 2.1 Å and the torsion angle Cys 69-C^{β}-S^{γ}-S^{γ}-C^{β}-BME is −71.8°. In addition, the hydroxyl group of this BME molecule forms a hydrogen bond (3.0 Å) to the one of the four oxygens of a sulfate ion bound to a symmetry-related protein molecule in the crystal. This interaction is probably of significance for crystal packing and may explain the need for BME in the crystallization medium. In principle this interaction might stabilize the binding of sulfate but is probably not of significance because a sulfate ion has been observed at the same site in the structure of hbFGF solved in a different crystal form in the absence of BME (Zhang et al., 1991).

The sulfur of Cys 92 appears to occupy two alternatives, defined as $S^{\gamma 1}$ and $S^{\gamma 2}$, with $\chi 1$ values of −42.3°

(g^+) and 27.0° (g^-), respectively. Extra electron density was observed in the vicinity of the $S^{\gamma 2}$ atom, extending toward bulk solvent. This density was interpreted and refined as a BME molecule with an occupancy of 0.5, i.e., the same occupancy as the $S^{\gamma 2}$ atom. The distance between the two sulfur atoms is 2.0 Å. However, except for the electron-dense sulfur atom, the remaining BME atoms are not well defined and have high temperature factors. This part of the bFGF molecule, which includes residues 87–89 and is situated in a mobile loop, is very flexible. The torsion value for Cys 92 (g^-)-C^{β}-S^{γ}-S^{γ}-C^{β}-BME is 58.1°.

Both BME molecules described above were also observed in the electron density maps of the selenate-treated crystals of hbFGF. This is somewhat surprising because crystals have a relatively high pH of 8.1 and were thoroughly washed in the absence of reducing agent before they were soaked with the ammonium selenate solution (otherwise a precipitate formed).

It has recently been shown that the two nonconserved cysteines of bFGF from bovine pituitaries, Cys 69 and Cys 87, are S-thiolated with glutathione (Thompson, 1992). In addition these two nonconserved cysteines are also blocked by carboxymethyl groups if the protein is treated with iodoacetic acid (Caccia et al., 1992). The formation of an adduct between BME and Cys 69, indicated by the electron density maps, is consistent with the accessibility of this residue to other ligands. Cys 87 is situated in a loop and is within a very flexible part of the molecule (Fig. 2). Because of this flexibility it is possible that Cys 87 reacts or partially reacts with BME, but this cannot be visualized in the electron density map. In the case of Cys 92, however, the crystallographic data suggest that this cysteine is at least partially accessible to BME, whereas the modification studies suggest no such availability.

Heparin binding

Both aFGF and bFGF have a high affinity for heparin, a naturally occurring highly sulfated glycosaminoglycan. Heparin has been shown to modify the activity of FGFs (Uhlrich et al., 1986; Neufeld et al., 1987) and to protect them from heat and acid inactivation (Gospodarowicz & Cheng, 1986) and from proteolytic digestion (Baird et al., 1988; Rosengart et al., 1988; Saksela et al., 1988; Damon et al., 1989).

We have previously reported that a sulfate ion, present in the crystallization medium, binds to the surface of hbFGF forming hydrogen bonds to the side chains of Lys 27, Arg 120, and Lys 125 as well as to the main-chain nitrogen atom of Arg 120. This immediately suggested that these residues might also be involved in heparin binding (Eriksson et al., 1991). The refined structure at 1.6 Å resolution confirms the interactions between the sulfate ion and the protein. These are illustrated in Figure 4 and Kinemage 3. In addition to interactions with the protein, two of the sulfate oxygens (O_1 and O_2) form hydrogen bonds to two water molecules (2.9 Å and 2.8 Å). The third sulfate oxygen, O_3, forms a hydrogen bond (3.0 Å) to the hydroxyl group of a symmetry-related BME molecule. The side chain of Arg 120 is not perfectly defined and the electron density suggests two alternative conformations. In one conformation (Fig. 4) a single hydrogen bond is made to the bound sulfate ion. When modeled in its second position, both N^{ϵ} and $N^{\eta 1}$ of the guanido group are within hydrogen bonding distance (Fig. 5).

Reductive methylation of lysine residues in aFGF has previously suggested the conserved Lys 125 as having a role in heparin binding (Harper & Lobb, 1988). Site-directed replacement of Lys 125 with glutamic acid also causes significant reduction in heparin binding (Burgess et al., 1990b). Thus there now exists ample evidence that Lys 125 is involved in heparin binding.

Nevertheless, to verify the binding of sulfate to the protein, the structure of hbFGF was solved using crystals in which the sulfate ions were replaced by the more electron-dense selenate ions. Interestingly, in this structure of hbFGF, two binding sites for selenate ions were identified. The first selenate binding site is identical with the previously identified sulfate binding site and confirms the earlier result. The second, unexpected site is about 6 Å from the first. The hydrogen bonding interactions formed by the second selenate ion are illustrated in Figure 5. Two of its oxygens are liganded by the side chains of Arg 120 and Lys 135. Another oxygen is 2.4 Å from the N^{ζ} atom of Lys 52 of a symmetry-related molecule. It should be noted, however, that no electron density is observed for the C^{δ} and N^{ζ} atoms of Lys 52 so these positions are not well defined. Glu 59, from the same symmetry-related molecule as Lys 52, is situated such that both its side-chain oxygens are only 2.9 Å from two of the selenate oxygens (Fig. 5). The presence of the two negative charges in such close proximity is presumably unfavorable and might explain, at least in part, why the occupancy of the selenate ion at this site is incomplete (about 60%). In solution, the "symmetry-related" Glu 59 would be absent from the second selenate binding site so that binding in solution might be enhanced relative to that observed in the crystal. As mentioned previously, the side chain of Arg 120 has two conformations in the 1.6-Å (sulfate) structure. In the ammonium selenate structure, however, the side chain of Arg 120 adopts the second of its two possible conformers, which permits simultaneous hydrogen bonds to both selenate ions (Fig. 5). In the sulfate-containing structure this conformation permits hydrogen bonds only to the original sulfate ion.

Why a sulfate ion is not observed at the second selenate binding site is not clear. There is no indication in the refined 1.6-Å structure that this is a potential sulfate binding site. Indeed, there is not even a solvent molecule seen at this site. As noted, however, the incomplete occupancy suggests that the affinity for selenate is weak. Also a sul-

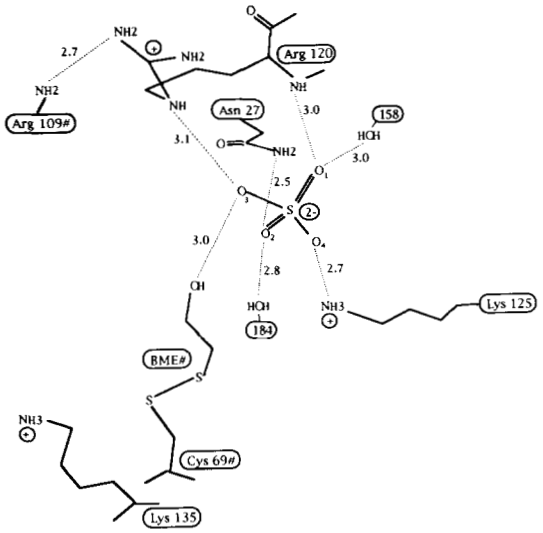

Fig. 4. Schematic drawing illustrating the binding of the single sulfate ion to hbFGF. Hydrogen bonds are indicated by dotted lines. Residues belonging to a symmetry-related molecule in the crystal lattice are identified with the symbol #. BME is a molecule of β-mercaptoethanol bound to Cys 69 in a symmetry-related molecule. The guanidinium groups of Arg 109 of one FGF molecule and Arg 120 of a symmetry-related molecule are within hydrogen-bonding distance, although we are not sure of the nature of this interaction. The geometry is shown in Figure 6.

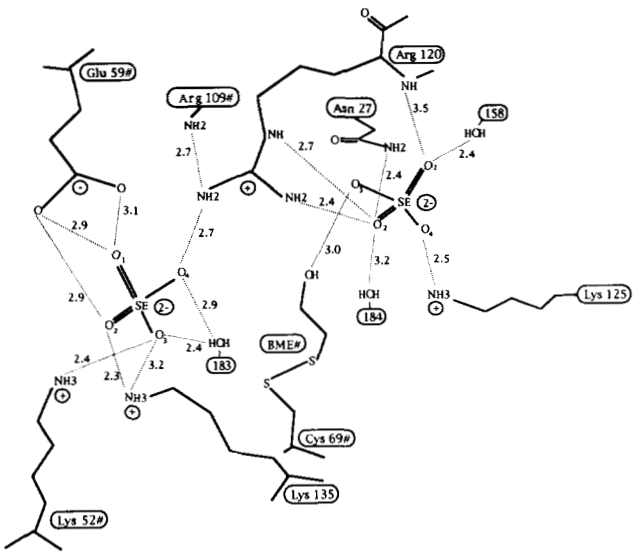

Fig. 5. Schematic drawing illustrating the binding of two selenate ions to hbFGF. Conventions as in Figure 4.

fate ion is about 0.2 Å smaller in diameter than selenate and so may not bridge as well from one FGF molecule to another in the crystal lattice (Fig. 5).

The presence of two closely spaced anionic binding sites on bFGF does suggest that both might participate in the binding of heparin. Heparin is a mixture of highly sulfated glycosaminoglycans, and there is no stereochemical reason why a molecule of heparin could not simultaneously occupy the twin anionic binding sites on the surface of bFGF.

Methods

Native structure in ammonium sulfate

Protein purification and crystallization were as described (Shing et al., 1984; Barr et al., 1988; Eriksson et al., 1991; Zhang et al., 1991). The crystals grow in the triclinic space group P1 with the unit cell $a = 30.9$ Å, $b = 33.4$ Å, $c = 35.9$ Å, $\alpha = 59.5°$, $\beta = 72.0°$, and $\gamma = 75.6°$. Initial crystals were grown at pH 8.1 by vapor diffusion from 2.0 M $(NH_4)_2SO_4$, 0.1 M Tris-HCl, pH 8.1, 0.1 M NaCl, and 0.1% (v/v) BME. However, the success of this project was made possible by the improvement of crystal quality by macroseeding (Eriksson et al., 1991).

The structure was initially solved using multiple isomorphous replacement and refined using the TNT least-squares refinement program package (Tronrud et al., 1987) to an R-factor of 17.4% including data from 20.0–2.2 Å resolution (Eriksson et al., 1991). A native data set to 1.6 Å resolution has now been collected on a Xuong-Hamlin area detector (Xuong et al., 1985) using graphite-monochromated CuKα radiation from a Rigaku RU200 rotating anode. Initially, both detectors were placed such that only reflections between 3.0 and 1.6 Å were collected. Each frame was 0.13°, and counts were accumulated for 40 s per frame. Data collection then continued at 13 s/frame, including lower resolution data. R_{merge}[1] for this data set was 2.7%. To obtain a complete low-resolution data, 46,606 observations from the 1.6-Å and the initial 2.2-Å data sets were combined to give 13,971 unique reflections (90% complete at 1.6 Å resolution) with R_{merge} of 4.0%.

Starting with the previous model (Eriksson et al., 1991), a total of 11 rounds of "conjugate direction" TNT refinement (Tronrud et al., 1987; Tronrud, 1992) were then performed, interrupted by manual inspection of the model against $2|F_o| - |F_c|$ and $|F_o| - |F_c|$ electron density maps, calculated with phases from the present model. Maps and coordinates were visualized on an Evans and Sutherland graphics display using the program FRODO (Jones, 1982). Each round of TNT refinement typically included four cycles of "loose weights" refinement where the model was allowed to relax its geometry to about 0.06–0.1 Å rms deviation in bond lengths. Then followed an additional four to six cycles of refinement with weights that constrained the bond length deviation to 0.02–0.017 Å rms. The model was then inspected manually on the display. During the first four rounds of refinement the higher

[1] $R_{merge} = \Sigma_{hkl} \Sigma_j |I_j - \langle I \rangle| / \Sigma \langle I \rangle$ for multiple measurements (i) from the same crystal.

resolution data were added stepwise: 20–1.9 Å, 20–1.8 Å, and 20–1.6 Å. After these four rounds the R-factor was 17.8%. During the remaining seven rounds of refinement, only minor corrections had to be made to the model.

The crystallographic R-factor for the fully refined model of hbFGF is 16.1% for all reflections observed between 20.0 and 1.6 Å resolution. Stereochemical deviations from ideal values are 0.016 Å and 2.7° for bond lengths and bond angles, respectively. Not included in the final model are residues 1–19 at the N-terminus and residues 144–146 at the C-terminus. Although residues 1–19 cannot be seen in the electron density maps, their presence in the crystals was verified by Edman degradation using protein from dissolved crystals (data not shown). It was, however, possible to include in the model the three amino acids, residues 87–89, that were unclear in the electron density maps calculated at 2.2 Å resolution (Eriksson et al., 1991). The final model of hbFGF at 1.6 Å resolution includes one bound sulfate ion, two BME molecules attached to Cys 69 and Cys 92, respectively, and 70 water molecules. A sample region of electron density from the final $2|F_o| - |F_c|$ map is shown in Figure 6.

The mean temperature factor is 25.7 Å^2 for all protein atoms (18.4 Å^2 and 32.8 Å^2 for main-chain and side-chain atoms only, respectively), 39.2 Å^2 for the sulfate ion, and 30.5 Å^2 and 67.6 Å^2 for the BME molecules situated at Cys 69 and Cys 92, respectively. However, the carbinol group of the latter BME molecule has temperature factors exceeding the cutoff value of 100 Å^2, indicating that it is very mobile.

The electron density suggests that both Cys 92 and Arg 120 display alternative conformations. The latter residue is of special interest because it participates in sulfate binding. The side chain of Cys 92 was refined assuming an equal distribution between the g^+ and g^- rotamers (Janin et al., 1978). The temperature factors of S^γ in the alternative conformations are 17.2 and 28.7 Å^2, respectively. BME can only bind to Cys 92 when its side chain adopts the g^- rotamer. Therefore this BME molecule was refined at half occupancy as well.

All 70 water molecules included in the model have B-factors less than 62 Å^2. The average temperature factors for the main-chain atoms as well as for the side-chain atoms of each residue are shown in Figure 7. Side chains with no or only weak electron density are listed in Table 1. The coordinates have been deposited in the Brookhaven Protein Data Bank.

Structure in ammonium selenate

Crystals of hbFGF were thoroughly washed in the above-described crystallization solution but without the reducing agent BME. They were then transferred to 3.0 M $(NH_4)_2SeO_4$, 0.1 M Tris-HCl, pH 8.1, and 0.1 M NaCl. The crystals were stored for 3–4 days, during which time the ammonium selenate solution was changed frequently. A total of 10,706 observations within 20.0–2.2 Å resolution were collected from a single selenium-soaked crystal using the Xuong–Hamlin area detector. The final data set includes 5,018 unique reflections (83% of all reflections possible to 2.2 Å) with an R_{merge} of 5.3%. The cell dimensions for the Se-soaked crystal were $a = 30.8$ Å, $b = 33.5$ Å, $c = 35.8$ Å, $\alpha = 58.8°$, $\beta = 72.4°$, and $\gamma = 76.1°$.

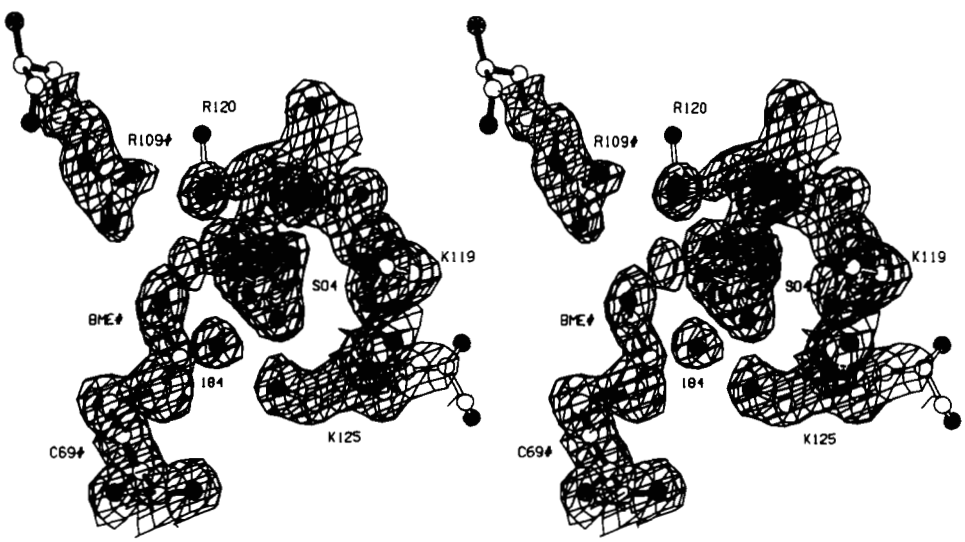

Fig. 6. Electron density map (coefficients $2|F_o| - |F_c|$; phases from the final refined model) in the vicinity of the sulfate binding site, superimposed on the refined structural model. Residues belonging to a symmetry-related molecule in the crystal lattice are identified with the symbol # and have solid bonds. Oxygen atoms are drawn as solid circles, nitrogens as half-solid circles, and carbons as open circles. Resolution is 1.6 Å. Contours are drawn at a level of 1σ, where σ is the rms density throughout the unit cell. BME is β-mercaptoethanol bound to Cys 69 in the symmetry-related molecule.

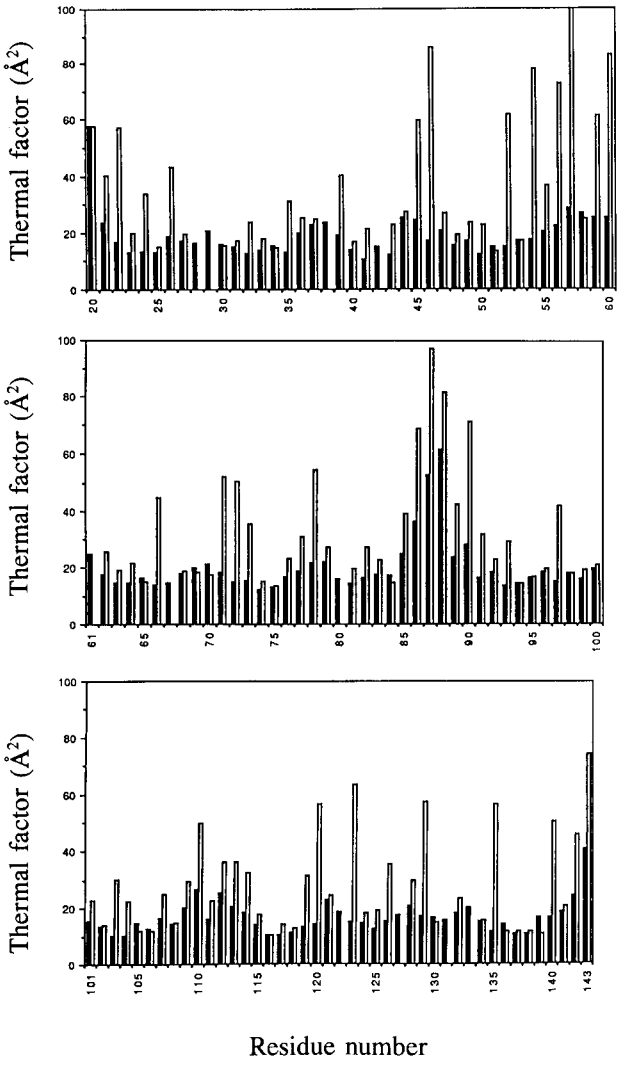

Fig. 7. Crystallographic thermal factors (B) for the hbFGF polypeptide chain plotted as a function of residue number. The mean main-chain and side-chain B-values are represented by the solid and open bars, respectively.

The isomorphous differences, R_{isom},[2] between the selenium data set and the 1.6-Å native data is 16.0%.

An initial ($F_{Se} - F_{native}$) electron density map was calculated with phases from the refined native model. This map contained three major peaks of height 7–8σ where σ is the rms density. The first peak (Fig. 8A) was at the site of the previously inferred sulfate ion, confirming its identity and its location. The second peak (also Fig. 8A) was 5.8 Å from the first and was in the vicinity of Lys 135 and Arg 120. The third highest peak was situated at another face of the molecule, 2.3 Å from water molecule 165 and in the vicinity of Lys 77, Glu 78, and Glu 91 (Fig. 8B).

[2] $R_{isom} = \Sigma_{hkl} \Sigma |F_{Se} - F_{native}| / \Sigma F_{native}$, where F_{Se} and F_{native} are structure factors from the selenium-soaked and the native data sets, respectively.

Table 1. *Atoms in side chains of hbFGF with no or only weak electron density*[a]

Residue number	No density	Weak density
Arg 22	$N^{\eta 1}$	
Lys 46	C^{γ}, C^{δ}, C^{ϵ}, N^{ζ}	
Lys 52	C^{δ}, C^{ϵ}	N^{ζ}
Gln 54		Whole side chain
Gln 56		C^{γ}, C^{δ}, $N^{\epsilon 2}$
Ala 57	C^{β}	
Lys 86	C^{δ}, C^{ϵ}	
Cys 87		C^{β}, S^{γ}
Val 88	$C^{\gamma 2}$	
Asp 90	$O^{\delta 2}$	
Arg 120	$N^{\eta 1}$, $N^{\eta 2}$	C^{ζ}
Gln 123		C^{δ}, $N^{\epsilon 2}$
Lys 129	C^{ϵ}, N^{ζ}	
Lys 135	C^{ϵ}, N^{ζ}	
Leu 140	$C^{\delta 2}$	

[a] In addition to the side-chain atoms listed in this table, no interpretable electron density is seen for residues 1–19 at the N-terminus and 144–146 at the C-terminus.

It was clear that the first peak corresponded to the replacement of a bound sulfate with a bound selenate ion. However, the interpretation of the second and the third peak was not as straightforward. It seemed plausible that both these peaks might correspond either to bound water molecules or to selenate ions. The structure was therefore independently refined with either selenate or water molecules at the two positions. With a fully occupied water molecule refined at the second site, calculated $|F_o| - |F_c|$ maps showed residual positive electron density. In addition the thermal factor tended to become negative, also indicating the presence of a more electron dense object at this site. From such experiments it is inferred that a selenate ion is bound at the second site, although with less than 100% occupancy. The third peak was interpreted and refined as corresponding to a fully-occupied water molecule (number 224) although it cannot be excluded that this "water molecule" might be a third selenate ion bound with low occupancy. There exist two positively charged residues in the vicinity, Lys 77 and the symmetry-related Lys 46 from a different FGF molecule. However, there are also two negatively charged residues nearby, Glu 78 and Glu 91.

The final model of the hbFGF-selenate complex has an R-factor of 13.8% for all data to 2.2 Å resolution with rms deviations from ideal values in bond lengths and bond angles of 0.018 Å and 3.2°, respectively.

Acknowledgments

We are most grateful to Drs. Steve Rosenberg and Pablo Valenzuela of Chiron Corporation for facilitating the project and for helpful advice. We also thank Drs. Larry Weaver, Steve Roder-

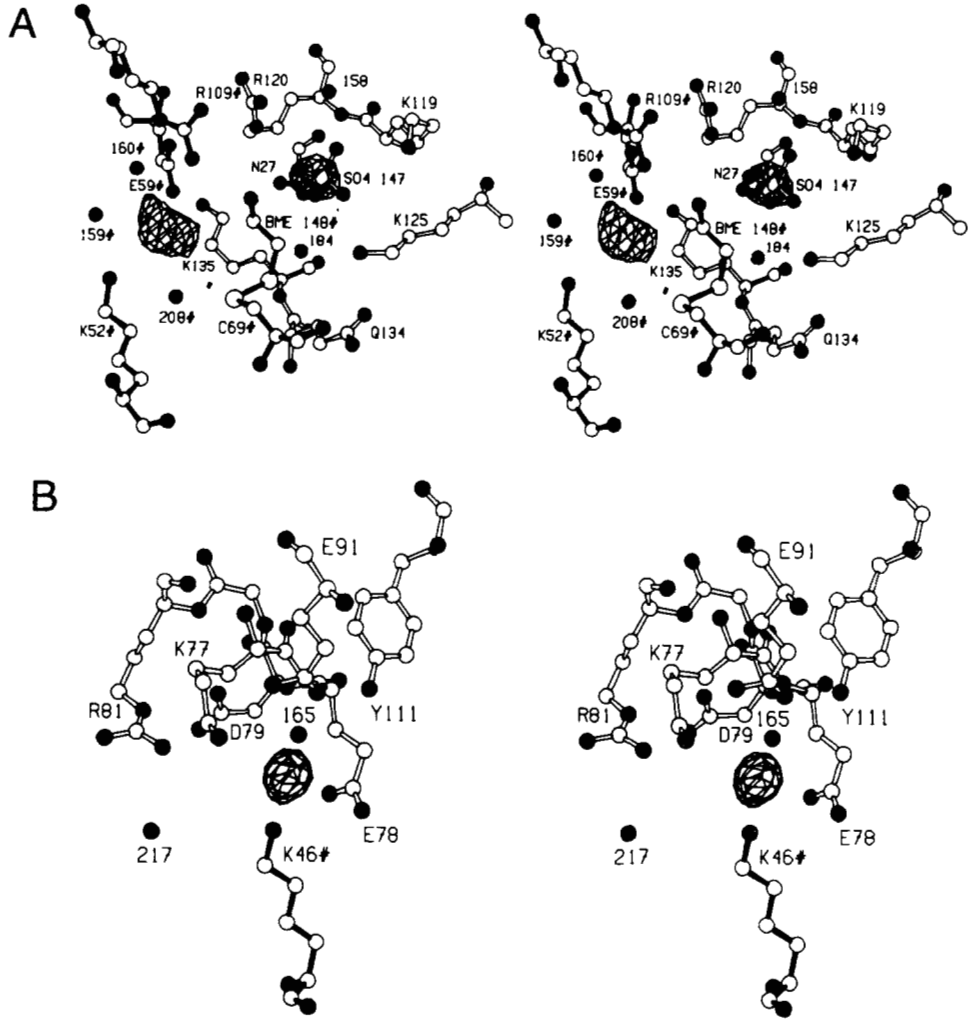

Fig. 8. A: Map showing the difference in electron density between the selenium-soaked and sulfate-soaked (native) crystals of hbFGF in the vicinity of the sulfate binding site. Amplitudes ($F_{Se} - F_{native}$), where F_{Se} and F_{native} are the observed structure amplitudes for the selenium and sulfate structure; phases calculated from the refined 1.6-Å model of hbFGF in sulfate. Residues belonging to a symmetry-related molecule have solid bonds and are identified by the symbol #. Oxygen atoms are drawn as solid circles, nitrogens as half-solid circles, and carbon as open circles. Resolution is 2.2 Å. Positive contours drawn at $+4.0\sigma$, where σ is the rms density throughout the unit cell. **B:** Map showing the difference in electron density between the selenium-soaked and sulfate-soaked (native) crystals of hbFGF in the vicinity of Lys 77, Glu 78, and Glu 91. All conventions as in Figure 8A.

ick, Dale Tronrud, and Jim Remington for help with the crystallography. A.E.E. acknowledges the support of the Swedish Natural Science Research Council. This work was supported in part by grants from the National Institutes of Health (GM20066) and the Lucille P. Markey Charitable Trust.

References

Abraham, J.A., Whang, J.L., Tumolo, A., Mergia, A., Friedman, J., Gospodarowicz, D., & Fiddes, J.C. (1986). Human basic fibroblast growth factor: Nucleotide sequence and genomic organization. *EMBO J. 5*, 2523–2528.

Ago, H., Kitagawa, Y., Fujishima, A., Matsuura, Y., & Katsube, Y. (1991). Crystal structure of basic fibroblast growth factor at 1.6 Å resolution. *J. Biochem. 110*, 360–363.

Baird, A. & Klagsbrun, M. (1991). Meeting review: The fibroblast growth factor family. *Cancer Cells 3*, 239–244.

Baird, A., Schubert, D., Ling, N., & Guillemin, R. (1988). Receptor- and heparin-binding domains of basic fibroblast growth factor. *Proc. Natl. Acad. Sci. USA 85*, 2324–2328.

Barr, P.J., Cousens, L.S., Lee-Ng, C.T., Medina-Selby, A., Masiarz, F.R., Hallewell, R.A., Chamberlain, S.H., Bradley, J.D., Lee, D., Steimer, K.S., Poulter, L., Burlingame, A.L., Esch, F., & Baird, A. (1988). Expression and processing of biologically active fibroblast growth factors in the yeast *Saccharomyces cerevisiae*. *J. Biol. Chem. 263*, 16471–16478.

Burgess, W.H., Dionne, C.A., Kaplow, J., Mudd, R., Friesel, R., Zilberstein, A., Schlessinger, J., & Jaye, M. (1990a). Characterization and cDNA cloning of phospholipase C-γ, a major substrate for heparin-binding growth factor 1 (acidic fibroblast growth factor)-activated tyrosine kinase. *Mol. Cell. Biol. 10*, 4770–4777.

Burgess, W.H. & Maciag, T. (1989). The heparin-binding (fibroblast) growth factor family of proteins. *Annu. Rev. Biochem. 58*, 575–606.

Burgess, W.H., Shaheen, A.M., Ravera, M., Jaye, M., Donohue, P.J., & Winkles, J.A. (1990b). Possible dissociation of the heparin-binding and mitogenic activities of heparin-binding (acidic fibroblast)

growth factor-1 from its receptor-binding activities by site-directed mutagenesis of a single lysine residue. *J. Cell Biol. 111*, 2129–2138.

Caccia, P., Nitti, G., Cletini, O., Pucci, P., Ruoppolo, M., Bertolero, F., Valsasina, B., Roletto, F., Cristiani, C., Cauet, G., Sarmientos, P., Malorni, A., & Marino, G. (1992). Stabilization of recombinant human basic fibroblast growth factor by chemical modifications of cysteine residues. *Eur. J. Biochem. 204*, 649–655.

Coughlin, S.R., Barr, P.J., Cousens, L.S., Fretto, L.J., & Williams, L.T. (1988). Acidic and basic fibroblast growth factors stimulate tyrosine kinase activity in vivo. *J. Biol. Chem. 263*, 988–993.

Damon, D.H., Lobb, R.R., D'Amore, P.A., & Wagner, J.A. (1989). Heparin potentiates the action of acidic fibroblast growth factor by prolonging its biological half-life. *J. Cell. Physiol. 138*, 221–226.

Delli-Bovi, P., Curatola, A.M., Kern, F.G., Greco, A., Ittmann, M., & Basilico, C. (1987). An oncogene isolated by transfection of Kaposi's sarcoma DNA encodes a growth factor that is a member of the FGF family. *Cell 50*, 729–737.

Dickson, C. & Peters, G. (1987). Potential oncogene product related to growth factors [letter]. *Nature 326*, 833.

Einspahr, H.M., Clancy, L.L., Holland, D.R., Muchmore, S.W., Watenpaugh, K.D., & Finzel, B.C. (1990). The crystal structure of human interleukin-1α. In *Current Research in Protein Chemistry* (Villafranca, J.J., Ed.), pp. 351–358. Academic Press, New York.

Eriksson, A.E., Cousens, L.S., Weaver, L.H., & Matthews, B.W. (1991). Three-dimensional structure of human basic fibroblast growth factor. *Proc. Natl. Acad. Sci. USA 88*, 3441–3445.

Esch, F., Baird, A., Ling, N., Ueno, N., Hill, F., Denoroy, L., Klepper, R., Gospodarowicz, D., Böhlen, P., & Guillemin, R. (1985). Primary structure of bovine pituitary basic fibroblast growth factor (FGF) and comparison with the amino-terminal sequence of bovine brain acidic FGF. *Proc. Natl. Acad. Sci. USA 82*, 6507–6511.

Finch, P.W., Rubin, J.S., Miki, T., Ron, D., & Aaronson, S.A. (1989). Human KGF is FGF-related with properties of a paracrine effector of epithelial cell growth. *Science 245*, 752–755.

Finzel, B.C., Clancy, L.L., Holland, D.R., Muchmore, S.W., Watenpaugh, K.D., & Einspahr, H.M. (1989). Crystal structure of recombinant human interleukin-1β at 2.0 Å resolution. *J. Mol. Biol. 209*, 779–791.

Folkman, J. & Klagsbrun, M. (1987). Angiogenic factors. *Science 235*, 442–447.

Friesel, R., Burgess, W.H., & Maciag, T. (1989). Heparin-binding growth factor 1 stimulates tyrosine phosphorylation in NIH 3T3 cells. *Mol. Cell. Biol. 9*, 1857–1865.

Gimenez-Gallego, G., Rodkey, J., Bennett, C., Rios-Candelore, M., DiSalvo, J., & Thomas, K. (1985). Brain-derived acidic fibroblast growth factor: Complete amino acid sequence and homologies. *Science 230*, 1385–1388.

Gospodarowicz, D. & Cheng, J. (1986). Heparin protects basic and acidic FGF from inactivation. *J. Cell. Physiol. 128*, 475–484.

Graves, B.J., Hatada, M.H., Hendrickson, W.A., Miller, J.K., Madison, V.S., & Satow, Y. (1990). Structure of interleukin 1α at 2.7 Å resolution. *Biochemistry 29*, 2679–2684.

Habazettl, J., Gondol, D., Wiltscheck, R., Otlewski, J., Schleicher, M., & Holak, T.A. (1992). Structure of the hisactophilin is similar to interleukin-1β and fibroblast growth factor. *Nature 359*, 855–858.

Harper, J.W. & Lobb, R.R. (1988). Reductive methylation of lysine residues in acidic fibroblast growth factor: Effect on mitogenic activity and heparin affinity. *Biochemistry 27*, 671–678.

Huang, S.S., Huang, J.S., & Kuo, M.-D. (1986). Association of bovine brain-derived growth factor receptor with protein tyrosine kinase activity. *J. Biol. Chem. 261*, 9568–9571.

Janin, J., Wodak, S., Levitt, M., & Maigret, B. (1978). Conformation of amino acid side-chains in proteins. *J. Mol. Biol. 125*, 357–386.

Jaye, M., Howk, R., Burgess, W., Ricca, G.A., Chiu, I.-M., Ravera, M.W., O'Brien, S.J., Modi, W.S., Maciag, T., & Drohan, W.N. (1986). Human endothelial cell growth factor: Cloning, nucleotide sequence, and chromosome localization. *Science 233*, 541–545.

Jones, T.A. (1982). FRODO: A graphics fitting program for macromolecules. In *Computational Crystallography* (Sayre, D., Ed.), pp. 303–317. Oxford University Press, Oxford, UK.

Kabsch, W. & Sanders, C. (1983). Dictionary of protein secondary structure: Pattern recognition of hydrogen-bonded and geometrical features. *Biopolymers 22*, 2577–2637.

Kan, M., Wang, F., Xu, J., Crabb, J.W., Hou, J., & McKeehan, W.L. (1993). An essential heparin-binding domain in the fibroblast growth factor receptor kinase. *Science 259*, 1918–1921.

Kimelman, D., Abraham, J.A., Haaparanta, T., Palisi, T.M., & Kirschner, M. (1988). Characterization of the HST-related FGF.6 gene, a new member of the fibroblast growth factor family. *Science 242*, 1053–1056.

Kraulis, P.J. (1991). MOLSCRIPT: A program to produce both detailed and schematic plots of protein structures. *J. Appl. Crystallogr. 24*, 946–950.

Maciag, T., Mehlman, T., Friesel, R., & Schreiber, A.B. (1984). Heparin binds endothelial cell growth factor, the principal endothelial cell mitogen in bovine brain. *Science 225*, 932–934.

Marics, I., Adelaide, J., Raybaud, F., Mattei, M.G., Coulier, F., Planche, J., de Lapeyriere, O., & Birnbaum, D. (1989). The presence of fibroblast growth factor in the frog egg: Its role as a natural mesoderm inducer. *Oncogene 4*, 335–340.

McLachlan, A.D. (1979). Three-fold structural pattern in the soybean trypsin inhibitor (Kunitz). *J. Mol. Biol. 133*, 557–563.

Miki, T., Bottaro, D.P., Fleming, T.P., Smith, C.L., Burgess, W.H., Chan, A.M.-L., & Aaronson, S.A. (1992). Determination of ligand-binding specificity by alternative splicing: Two distinct growth factor receptors encoded by a single gene. *Proc. Natl. Acad. Sci. USA 89*, 246–250.

Murzin, A.G., Lesk, A.M., & Chothia, C. (1992). β-Trefoil fold. Patterns of structure and sequence in the Kunitz inhibitors interleukins-1β and 1α and fibroblast growth factors. *J. Mol. Biol. 223*, 531–543.

Musci, T.J., Amaya, E., & Kirschner, M.W. (1990). Regulation of the fibroblast growth factor receptor in early *Xenopus* embryos. *Proc. Natl. Acad. Sci. USA 87*, 8365–8369.

Neufeld, G. & Gospodarowicz, D. (1986). Basic and acidic fibroblast growth factors interact with the same cell surface receptors. *J. Biol. Chem. 261*, 5631–5637.

Neufeld, G., Gospodarowicz, D., Dodge, L., & Fujii, D.K. (1987). Heparin modulation of the neurotropic effects of acidic and basic fibroblast growth factors and nerve growth factor on PC12 cells. *J. Cell. Physiol. 131*, 131–140.

Nurcombe, V., Ford, M.D., Wildschut, J.A., & Bartlett, P.F. (1993). Developmental regulation of neural response to FGF-1 and FGF-2 by heparan sulfate proteoglycan. *Science 260*, 103–106.

Onesti, S., Brick, P., & Blow, D.M. (1991). Crystal structure of a Kunitz-type trypsin inhibitor from *Erythrina caffra* seeds. *J. Mol. Biol. 217*, 153–176.

Priestle, J.P., Schär, H.-P., & Grütter, M.G. (1988). Crystal structure of the cytokine interleukin-1β. *EMBO J. 7*, 339–343.

Priestle, J.P., Schär, H.-P., & Grütter, M.G. (1989). Crystallographic refinement of interleukin 1β at 2.0 Å resolution. *Proc. Natl. Acad. Sci. USA 86*, 9667–9671.

Rosengart, T.K., Johnson, W.V., Friesel, R., Clark, R., & Maciag, T. (1988). Heparin protects heparin-binding growth factor-I from proteolytic inactivation in vitro. *Biochem. Biophys. Res. Commun. 152*, 432–440.

Rossmann, M.G. & Argos, P. (1975). A comparison of the heme binding pocket in globins and cytochrome b_5. *J. Biol. Chem. 250*, 7525–7532.

Saksela, O., Moscatelli, D., Sommer, A., & Rifkin, D.B. (1988). Endothelial cell-derived heparan sulfate binds basic fibroblast growth factor and protects it from proteolytic degradation. *J. Cell Biol. 107*, 743–751.

Shing, Y., Folkman, J., Sullivan, R., Butterfield, C., Murray, J., & Klagsbrun, M. (1984). Purification of a tumor-derived capillary endothelial cell growth factor. *Science 223*, 1296–1299.

Shreiber, A.B., Kenney, J., Kowalski, W.J., Friesel, R., Mehlman, T., & Maciag, T. (1985). Interaction of endothelial cell growth factor with heparin: Characterization by receptor and antibody recognition. *Proc. Natl. Acad. Sci. USA 82*, 6138–6142.

Sweet, R.M., Wright, H.T., Janin, J., Chothia, C.H., & Blow, D.M. (1974). Crystal structure of the complex of porcine trypsin with soybean trypsin inhibitor (Kunitz) at 2.6 Å resolution. *Biochemistry 13*, 4212–4228.

Terranova, V.P., DiFlorio, R., Lyall, R.M., Hic, S., Friesel, R., & Maciag, T. (1985). Human endothelial cells are chemotactic to endothelial cell growth factor and heparin. *J. Cell Biol. 101*, 2330–2334.

Thomas, K.A. & Gimenez-Gallego, G. (1986). Fibroblast growth factors: Broad spectrum mitogens with potent angiogenic activity. *Trends Biochem. Sci. 11*, 81–84.

Thompson, S.A. (1992). The disulfide structure of bovine pituitary basic fibroblast growth factor. *J. Biol. Chem. 267*, 2269–2273.

Thornton, S.C., Mueller, S.N., & Levine, E.M. (1983) Human endothelial cells: Use of heparin in cloning and long-term serial cultivation. *Science 222*, 623–625.

Tronrud, D.E. (1992). Conjugate-direction minimization: An improved method for the refinement of macromolecules. *Acta Crystallogr. A 48*, 912–916.

Tronrud, D.E., Ten Eyck, L.F., & Matthews, B.W. (1987). An efficient general-purpose least-squares refinement program for macromolecular structures. *Acta Crystallogr. A 43*, 489–503.

Uhlrich, S., Lagente, O., Lenfant, M., & Courtois, Y. (1986). Effect of heparin on the stimulation of non-vascular cells by human acidic and basic FGF. *Biochem. Biophys. Res. Commun. 137*, 1205–1213.

Vainikka, S., Partanen, J., Bellosta, P., Coulier, F., Basilico, C., Jaye, M., & Alitalo, K. (1992). Fibroblast growth factor receptor-4 shows novel features in genomic structure, ligand binding and signal transduction. *EMBO J. 11*, 4273–4280.

Xuong, N.H., Nielsen, C., Hamlin, R., & Anderson, D. (1985). Strategy for data collection from protein crystals using a multiwire counter area detector diffractometer. *J. Appl. Crystallogr. 18*, 342–350.

Yoshida, T., Miyagawa, K., Odagiri, H., Sakamoto, H., Little, P.F.R., Terada, M., & Sugimura, T. (1987). Genomic sequence of *hst*, a transforming gene encoding a protein homologous to fibroblast growth factors and the *int-2*-encoded protein. *Proc. Natl. Acad. Sci. USA 84*, 7305–7309.

Zemke, K.J., Müller-Fahrnow, A., Jany, K.-D., Pal, G.P., & Saenger, W. (1991). The three-dimensional structure of the bifunctional proteinase K/α-amylase inhibitor from wheat (PKI3) at 2.5 Å resolution. *FEBS Lett. 279*, 240–242.

Zhan, X., Bates, B., Hu, X., & Goldfarb, M. (1988). The human FGF-5 oncogene encodes a novel protein related to fibroblast growth factors. *Mol. Cell. Biol. 8*, 3487–3495.

Zhang, J., Cousens, L.S., Barr, P.J., & Sprang, S.R. (1991). Three-dimensional structure of human basic fibroblast growth factor, a structural homolog of interleukin 1β. *Proc. Natl. Acad. Sci. USA 88*, 3446–3450.

Zhu, X., Komiya, H., Chirino, A., Faham, S., Fox, G.M., Arakawa, T., Hsu, B.T., & Rees, D.C. (1991). Three-dimensional structures of acidic and basic fibroblast growth factors. *Science 251*, 90–93.